JACS
JOURNAL OF THE AMERICAN CHEMICAL SOCIETY
Communication
pubs.acs.org/JACS

6,12-Diarylindeno[1,2-*b*]fluorenes: Syntheses, Photophysics, and Ambipolar OFETs

Daniel T. Chase,[†,§] Aaron G. Fix,[†] Seok Ju Kang,[‡] Bradley D. Rose,[†] Christopher D. Weber,[†] Yu Zhong,[‡] Lev N. Zakharov,[†] Mark C. Lonergan,[†] Colin Nuckolls,*[,‡] and Michael M. Haley*[,†]

[†]Department of Chemistry and Materials Science Institute, University of Oregon, Eugene, Oregon 97403-1253, United States
[‡]Department of Chemistry, Columbia University, New York, New York 10027, United States

Supporting Information

ABSTRACT: Herein we report the synthesis and characterization of a series of 6,12-diarylindeno[1,2-*b*]fluorenes (IFs). Functionalization with electron donor and acceptor groups influences the ability of the IF scaffold to undergo two-electron oxidation and reduction to yield the corresponding 18- and 22-π-electron species, respectively. A single crystal of the pentafluorophenyl-substituted IF can serve as an active layer in an organic field-effect transistor (OFET). The important finding is that the single-crystal OFET yields an ambipolar device that is able to transport holes and electrons.

Conjugated polycyclic hydrocarbons have been the subject of intense research over the last two decades for their potential use in a variety of materials applications such as organic light-emitting diodes, thin-film transistors, and solar cells.[1] Of particular interest is the indeno[1,2-*b*]fluorene (IF) skeleton (e.g., **1** and **2**, Figure 1), a 6−5−6−5−6 fused ring system that in its fully conjugated state closely resembles pentacene.[2] As IFs possess two fewer carbon atoms and hence two fewer π electrons than pentacenes, they could be considered as antiaromatic molecules. This definition remains a formality, however, as the internal core exhibits bond lengths and bond alternation resembling a dibenzo-fused *s*-indacene.[3] Furthermore, **1** and **2** are stable upon heating for prolonged periods (80 °C for **1**, 150 °C for **2**) without noticeable decomposition, a trait not typically associated with antiaromatic compounds. These observations of stability parallel those found with structurally similar dibenzopentalene derivatives.[4]

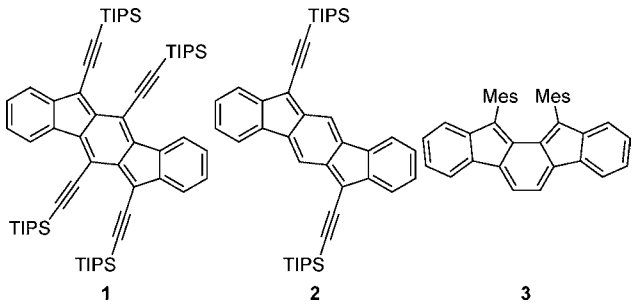

Figure 1. Fully conjugated indenofluorenes **1**−**3**.

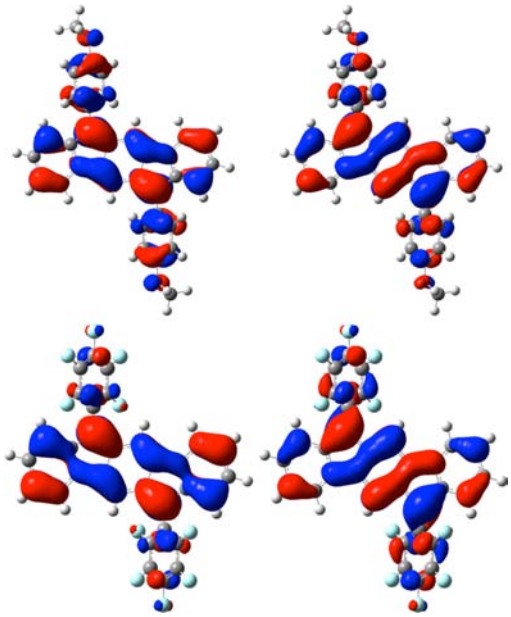

Figure 2. (left) HOMO and (right) LUMO plots for IFs **4b** (top) and **4j** (bottom).

We recently reported the synthesis and properties of a series of 2,8-disubstituted derivatives of **2**.[5] These compounds possess UV−vis profiles similar to that of **1** with slightly larger HOMO/LUMO gaps. As with our reported diynyl-IF-diones,[6] **2** and derivatives could accept two electrons in a quasi-reversible fashion, exhibiting LUMO energy levels comparable to or further from the vacuum level than that of the ubiquitous electron acceptor PCBM.[7] Furthermore, the solid-state structures of two derivatives showed one-dimensional π stacks with intermolecular distances as short as 3.40 Å, an improvement over the herringbone motif found for **1**. Functionalization at the 2- and 8-positions, however, had only a modest effect on the HOMO and LUMO energy levels, as calculations showed minimal orbital density at those positions. In addition to our studies, Tobe and Shimizu recently disclosed the synthesis of 11,12-dimesitylindeno[2,1-*a*]fluorene (**3**),[8] an isomeric IF species possessing physical characteristics similar to those of **1** and **2**.

Received: April 9, 2012
Published: June 14, 2012

dx.doi.org/10.1021/ja303402p | *J. Am. Chem. Soc.* 2012, 134, 10349−10352

Scheme 1. Synthesis of 6,12-Diarylindeno[1,2-*b*]fluorenes

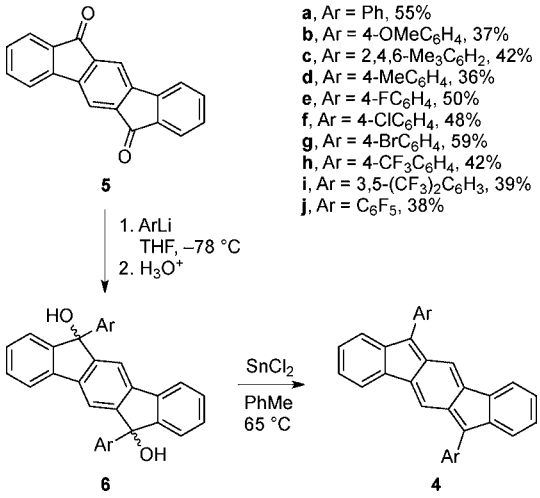

To expand further the versatility of the IF scaffold, we considered substitution motifs beyond the previously used triisopropylsilyl (TIPS)-substituted ethynyl moiety. Arylation at the 6- and 12-positions represents a logical next step, as arenes functionalized with either donor or acceptor groups might impart a more diverse range of IF optoelectronic properties. This supposition is supported by the calculated HOMO/LUMO plots in Figure 2, which show considerable orbital density at those positions. The synthesis of arylated IFs also fulfills a historic purpose in that one of the original IFs exhibiting full conjugation, 6,12-diphenyl-IF **4a**, was only briefly described by Scherf.[9] Herein we disclose the syntheses of IFs **4a–j** from readily available 6,12-indenofluorenedione (**5**),[10] along with the respective optical, electrochemical, and computational data. Importantly, we show that pentafluorophenyl derivative **4j** can be used to construct an organic field-effect transistor (OFET) that exhibits ambipolar behavior.

The same strategy for synthesizing **2** via dione **5**[10] can be readily applied to give **4a** (Scheme 1). Addition of lithiated bromobenzene gave crude diol **6a**, and subsequent reduction using $SnCl_2$ in toluene at 65 °C afforded a magenta solution from which the parent **4a** was obtained in 55% yield over two steps. This reaction scheme was then extended to the series of 6,12-diaryl-IFs **4b–j**, which were isolated in good to modest yields after recrystallization. The reduction was sluggish for strongly electron-deficient arenes such as **6h–j**, and the addition of a small amount of trifluoroacetic acid (similarly used for the synthesis of **3**)[8] was required for the reduction to occur smoothly.

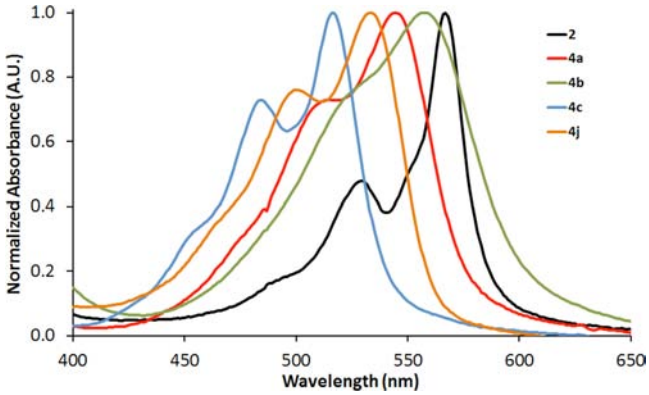

Figure 3. Electronic absorption spectra for IFs **2**, **4a–c**, and **4j**; all spectra were recorded in $CHCl_3$ at 15–25 μM.

Table 1 contains the UV–vis absorption data for all of the diaryl-IFs; individual spectra of **2**, **4a–c**, and **4j** are shown in Figure 3 [see the Supporting Information (SI) for the spectra of **4d–i**]. Like **2**, **4a** exhibits three low-energy absorptions (λ_{max} = 544 nm), but these are hypsochromically shifted by ca. 50 and 25 nm with respect to **1** and **2**. This can be attributed to the exchange of electron-withdrawing acetylenes with aryl groups, a consequence also observed with substituted pentacenes.[11] Variation of the aryl substituents at the 6- and 12-positions has a notable impact on the absorption profiles: methoxyphenyl-substituted **4b** exhibits a λ_{max} of 558 nm, while pentafluorophenyl-substituted **4j** has a λ_{max} of 533 nm. Interestingly, the mesityl derivative **4c** exhibits a λ_{max} of 516 nm, which is attributed to the nearly orthogonal orientation of the mesityl and IF

Table 1. Computational, Electrochemical, and Optical Data for Indeno[1,2-*b*]fluorenes 2 and 4a–j

	computational[a]			electrochemical[b]					optical[c]	
compd	E_{HOMO}	E_{LUMO}	E_{gap}	$E(A^+/A)$, $E(A^{2+}/A^+)$, $E(A^{3+}/A^{2+})$	$E(A/A^-)$, $E(A^-/A^{2-})$	E_{HOMO}	E_{LUMO}	E_{gap}	λ_{max}	E_{gap}[d]
2	−5.51	−3.47	2.04	1.20	−0.69, −1.20	−5.88	−4.00	1.88	568	2.12
4a	−5.24	−3.07	2.17	1.00, 1.31,[e] 1.51[e]	−0.96, −1.49[e]	−5.68	−3.72	1.96	544	2.17
4b	−5.00	−2.90	2.10	0.81, 1.07[e]	−1.01, −1.53[e]	−5.50	−3.68	1.82	558	2.05
4c	−5.34	−2.92	2.42	1.10, 1.59[e]	−1.12, −1.73[e]	−5.78	−3.56	2.22	516	2.29
4d	−5.13	−2.98	2.15	0.93, 1.21,[e] 1.48[e]	−0.99, −1.50[e]	−5.61	−3.69	1.92	550	2.12
4e	−5.37	−3.20	2.17	1.03, 1.24,[e] 1.52[e]	−0.93, −1.41[e]	−5.71	−3.76	1.95	543	2.16
4f	−5.42	−3.27	2.15	1.05, 1.30,[e] 1.53[e]	−0.88, −1.34[e]	−5.74	−3.81	1.93	548	2.14
4g	−5.43	−3.28	2.15	1.04, 1.38,[e] 1.51[e]	−0.89, −1.35[e]	−5.73	−3.80	1.93	550	2.12
4h	−5.65	−3.49	2.16	1.22, 1.41,[e], 1.54[e]	−0.84, −1.12	−5.91	−3.85	2.06	545	2.16
4i	−5.89	−3.73	2.16	1.35,[e] 1.67[e]	−0.73, −1.07	−6.05	−3.97	2.08	543	2.16
4j	−5.92	−3.71	2.21	1.49,[e] 1.66[e]	−0.68, −1.17	−6.17	−4.00	2.17	533	2.20

[a]Calculations were performed at the B3LYP/6-311+G** level of theory; energies are in eV. [b]CVs were recorded using 1–5 mM of analyte in 0.1 M Bu_4NOTf/CH_2Cl_2 at a scan rate of 50 mV/s with a glassy carbon working electrode, a Pt coil counter electrode, and a Ag wire pseudo-reference electrode. E is the half-wave potential ($E_{1/2}$) for reversible processes and the potential of the peak anodic or cathodic current (E_p) for irreversible processes. Potential values are reported in V vs SCE using the Fc^+/Fc couple (0.46 V) as an internal standard. HOMO and LUMO energy levels in eV were approximated using SCE = −4.68 eV vs vacuum (see ref 13) and $E_{1/2}$ values for reversible processes or E_p values for irreversible processes. [c]Spectra were obtained in $CHCl_3$; wavelengths are in nm. [d]The optical HOMO/LUMO gap was determined as the intersection of the x axis and a tangent line passing through the inflection point of the lowest-energy absorption; energies are in eV. [e]Irreversible wave.

dx.doi.org/10.1021/ja303402p | J. Am. Chem. Soc. 2012, 134, 10349–10352

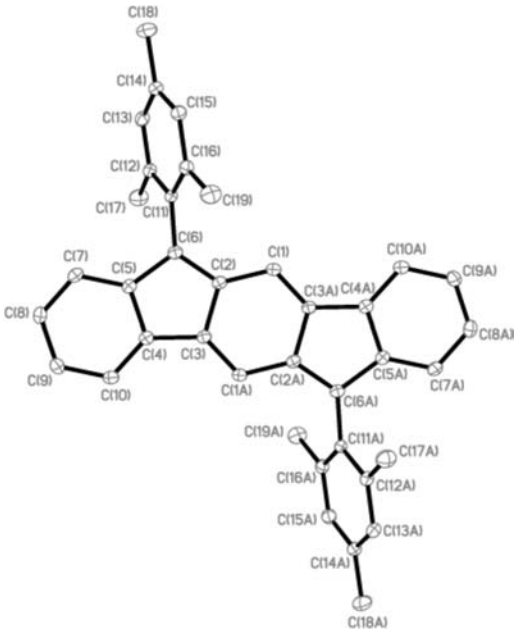

Figure 4. X-ray crystal structure of **4c**; H atoms have been omitted for clarity, and ellipsoids are drawn at the 30% probability level.

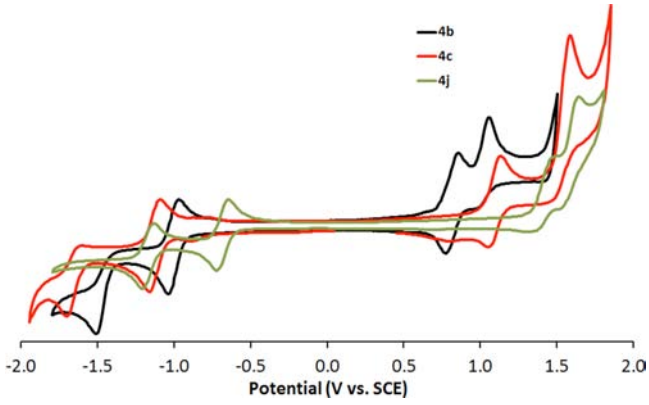

Figure 5. CVs for IFs **4b**, **4c**, and **4j**.

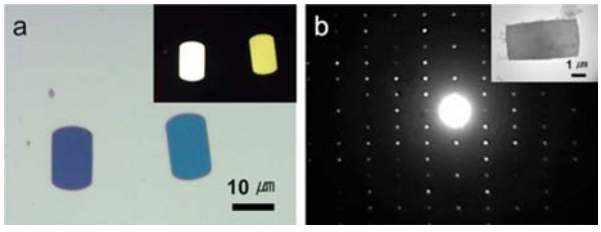

Figure 6. (a) OM of single crystals of **4j** prepared by a solvent-exchange method. The inset shows an OM with crossed polarizers. (b) SAED pattern and (inset) bright-field TEM image of a single crystal of **4j**.

enforced by the *o*-methyl groups. The X-ray structure of **4c** (Figure 4) corroborates this hypothesis, as the dihedral angle between the mesityl and indenofluorene rings is 72° (80.6° calculated dihedral). Thus, little electronic communication between the π systems exists in this instance, which effectively reduces the conjugation path length in **4c**, resulting in the hypsochromic shift. All of the other arylated IFs are predicted to exhibit more typical biphenyl dihedral angles[12] (calculated 43–45° for **4a–i**, 50.6° for **4j**), and their spectra more strongly reflect

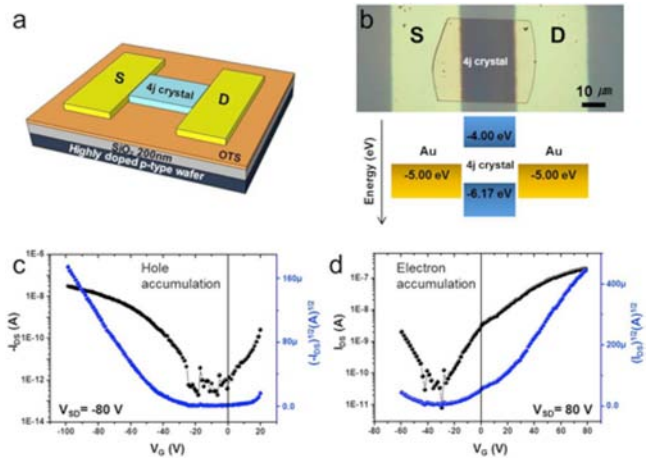

Figure 7. (a) Schematic of an OFET with an active channel consisting of a **4j** single crystal. (b) Top-view OM of an OFET (top) and energy diagram for Au/**4j** crystal/Au (bottom). (c, d) *I*–*V* transfer characteristics of OFETs with (c) negative and (d) positive drain voltages.

the effects of the aryl substituents, as noted above. As observed previously for **1** and **2**, IFs **4a–j** are nonemissive.

Cyclic voltammograms (CVs) for **4b**, **4c**, and **4j** are displayed in Figure 5 (see the SI for the CVs for **4a**, **4d–i**). All of the voltammetry data are compiled in Table 1, which shows the half-wave potentials ($E_{1/2}$) for reversible waves or the potential of peak current (E_p) for irreversible waves. $E_{1/2}$ is generally very close to the standard reduction potential. In solution, the neutral diaryl-IF scaffold exhibits quasi-reversible behavior in accepting up to two electrons in separate waves (A/A^- and A^-/A^{2-}). The $E_{1/2}(A/A^-)$ values for **4a–j** range from −0.68 to −1.12 V vs SCE, which in general are more negative than that observed for **2**. Electron-withdrawing groups shift $E_{1/2}$ to more positive values while electron-donating groups shift it to more negative values, as such groups work respectively to stabilize and destabilize the resulting anionic species. The wave for the second reduction (A^-/A^{2-}) was irreversible in most cases, although the E_p showed trends similar to those for $E_{1/2}(A/A^-)$. With the exception of **4i** and **4j**, the diaryl-IFs could be reversibly oxidized from their neutral states, an unanticipated trait on the basis of our previous observations for **1** and **2**. The $E_{1/2}(A^+/A)$ and $E_p(A^+/A)$ values for **4a–j** range from 0.81 to 1.49 V. Electron-withdrawing groups destabilize the resulting cationic species, while electron-donating groups provide the opposite effect. A second and sometimes third anodic peak (**4a** and **4d–h**) were observed for each compound at potentials more positive than $E_{1/2}(A^+/A)$, but these processes were irreversible. The trend noted for $E_{1/2}(A^+/A)$ was also observed for $E_p(A^{2+}/A^+)$ and for $E_p(A^{3+}/A^{2+})$ when it was present. As a whole, the HOMO and LUMO energy levels of **4a–j** span 0.7 and 0.4 eV ranges,[13] respectively, which is far beyond the 0.15 eV range demonstrated by **2** and derivatives.[5] *p*-Anisyl-IF **4b** displays $E_{1/2}$ values for the first reduction (−1.01 V) and oxidation (0.81 V) of its neutral form, which closely mirror those found for 6,13-bis(TIPS-ethynyl)pentacene, which are −1.10 and 0.74 V, respectively.[11,14]

Micron-scale single crystals of **4j** could be prepared using a solvent-exchange method.[15] Figure 6 displays an optical micrograph (OM) of these microcrystals on a silicon wafer with 200 nm of SiO_2 on its surface. The strong and uniform birefringence of **4j** along with the reflections observed in the selected-area electron diffraction (SAED) pattern and the bright-

dx.doi.org/10.1021/ja303402p | J. Am. Chem. Soc. 2012, 134, 10349–10352

field TEM image (Figure 6b) indicate that these microcrystals have a single-crystal orientation.

After growth of the crystal on the silicon wafer, OFETs with a microcrystal of **4j** as the active channel in the device were constructed.[16] Figure 7a is a schematic of such a device, and Figure 7b is an OM of a device.[17] To construct the device, the surface of the SiO_2 interface was passivated with a monolayer of octadecyltrichlorosilane. This treatment has been shown previously to reduce the trap sites at the dielectric−semiconductor interface.[18] The Au source and drain electrodes were thermally deposited through a TEM grid to form a top-contact bottom-gate transistor. The work function of Au is ca. 5.0 eV, meaning that both holes and electrons can be injected from Au into **4j** single crystals through the Schottky barrier at the metal−semiconductor contact.[19]

Figure 7c,d shows the transfer characteristics of the **4j** OFET measured in a N_2-filled glovebox. The transfer curves clearly exhibit ambipolar current modulation. The field-effect mobility was calculated from the slope of a plot of the square root of the drain current (I_{DS}) versus gate voltage (V_G) in the saturation regime. The field-effect mobility can be calculated using $I_{DS} = (W/2L)C_i\mu(V_G - V_T)^2$, where W and L are the width and length of the channel and C_i (=17.8 nF cm^{-2}), μ, and V_T correspond to the capacitance per unit area of the gate insulator, the field-effect mobility, and the threshold voltage, respectively. The field-effect hole and electron mobilities extracted from the **4j** single crystal ambipolar transistor are 7×10^{-4} and 3×10^{-3} cm^2 V^{-1} s^{-1} in the saturation regime, respectively.[20] The HOMO and LUMO levels of diaryl-IF **4j** create well-balanced ambipolar OFETs with Au electrodes because the work function of the electrodes is in the middle of the gap. Interestingly, there are very few ambipolar OFETs made from single crystals of organic semiconductors.[21]

In conclusion, we have prepared a family of 6,12-diarylindeno[1,2-*b*]fluorenes and shown that aryl substitution can significantly affect the redox properties of the molecules. In cyclic voltammetry experiments, the diaryl-IFs can either accept or donate two electrons. Pentafluorophenyl-substituted IF **4j** was utilized as the active element in a single-crystal OFET that exhibited ambipolar behavior with Au source/drain contacts. Future work will focus on additional indenofluorene topologies and molecule functionalization as well as further device studies.

■ ASSOCIATED CONTENT

Supporting Information

Experimental details, NMR and absorption spectra, CVs, and computational data for **4a−j**; CIF file for **4c**; OFET fabrication details for **4j**. This material is available free of charge via the Internet at http://pubs.acs.org.

■ AUTHOR INFORMATION

Corresponding Author

haley@uoregon.edu; cn37@columbia.edu

Present Address

[§]Department of Chemistry and Biochemistry, The University of Texas, Austin, Texas 78712.

Notes

The authors declare no competing financial interest.

■ ACKNOWLEDGMENTS

We thank the National Science Foundation (CHE-1013032) for support of this research and for instrumentation grant support (CHE-0923589). The electrochemical work was funded by the Division of Chemical Sciences, Geosciences, and Biosciences, Office of Basic Energy Sciences, U.S. Department of Energy through Grant DE-FG02-07ER15907. B.D.R. and C.D.W. acknowledge the NSF for GK-12 (DGE-0742540) and IGERT (DGE-0549503) Fellowships, respectively. C.N. thanks the DOE and S.J.K. thanks NSF-MIRT (DMR-1122594).

■ REFERENCES

(1) (a) *Functional Organic Materials*; Müller, T. J. J., Bunz, U. H. F., Eds.; Wiley-VCH: Weinheim, Germany, 2007. (b) *Organic Light Emitting Devices: Synthesis, Properties and Applications*; Mullen, K., Scherf, U., Eds.; Wiley-VCH: Weinheim, Germany, 2006. (c) *Carbon-Rich Compounds*; Haley, M. M., Tykwinski, R. R., Eds.; Wiley-VCH: Weinheim, Germany, 2006.

(2) (a) Anthony, J. E. *Chem. Rev.* **2006**, *106*, 5028. (b) Anthony, J. E. *Angew. Chem., Int. Ed.* **2008**, *47*, 452.

(3) Chase, D. T.; Rose, B. D.; Zakharov, L. N.; Haley, M. M. *Angew. Chem., Int. Ed.* **2011**, *50*, 1227.

(4) For example, see: (a) Saito, M.; Nakamura, M.; Tajima, T. *Chem.—Eur. J.* **2008**, *14*, 6062. (b) Kawase, T.; Konishi, A.; Hirao, Y.; Matsumoto, K.; Kurata, H.; Kubo, T. *Chem.—Eur. J.* **2009**, *15*, 2653. (c) Zerubba, U. L.; Tilley, T. D. *J. Am. Chem. Soc.* **2009**, *131*, 2796. (d) Zhang, H.; Karasawa, T.; Yamada, H.; Wakamiya, A.; Yamaguchi, S. *Org. Lett.* **2009**, *11*, 3076. (e) Saito, M. *Symmetry* **2010**, *2*, 950. (f) Zerubba, U. L.; Tilley, T. D. *J. Am. Chem. Soc.* **2010**, *132*, 11012. (g) Kawase, T.; Fujiwara, T.; Kitamura, C.; Konishi, A.; Hirao, Y.; Matsumoto, K.; Kurata, H.; Kubo, T.; Shinamura, S.; Mori, H.; Miyazaki, E.; Takimiya, K. *Angew. Chem., Int. Ed.* **2010**, *49*, 7728.

(5) Chase, D. T.; Fix, A. G.; Rose, B. D.; Weber, C. D.; Nobusue, S.; Stockwell, C. E.; Zakharov, L. N.; Lonergan, M. C.; Haley, M. M. *Angew. Chem., Int. Ed.* **2011**, *50*, 11103.

(6) Rose, B. D.; Chase, D. T.; Weber, C. D.; Zakharov, L. N.; Lonergan, M. C.; Haley, M. M. *Org. Lett.* **2011**, *13*, 2106.

(7) (a) Anthony, J. E.; Facchetti, A.; Heeney, M.; Marder, S. R.; Zhan, X. *Adv. Mater.* **2010**, *22*, 3876. (b) Dong, H.; Wang, C.; Hu, W. *Chem. Commun.* **2010**, *46*, 5211. (c) Mikroyannidis, J. A.; Kabanakis, A. N.; Sharma, S. S.; Sharma, G. D. *Adv. Funct. Mater.* **2011**, *21*, 746.

(8) Shimizu, A.; Tobe, Y. *Angew. Chem., Int. Ed.* **2011**, *50*, 6906.

(9) Reisch, H.; Wiesler, U.; Scherf, U.; Tuytuylkov, N. *Macromolecules* **1996**, *29*, 8204.

(10) Merlet, S.; Birau, M.; Wang, Z. Y. *Org. Lett.* **2002**, *4*, 2157.

(11) Kaur, I.; Jia, W.; Kopreski, R. P.; Selvarasah, S.; Dokmeci, M. R.; Pramanik, C.; McGruer, N. E.; Miller, G. P. *J. Am. Chem. Soc.* **2008**, *130*, 16274.

(12) Almenningen, A.; Bastiansen, O.; Fernholt, L.; Cyvin, B. N.; Cyvin, S. J.; Samdal, S. *J. Mol. Struct.* **1985**, *128*, 59.

(13) Reiss, H.; Heller, A. *J. Phys. Chem.* **1985**, *89*, 4207.

(14) 6,13-Bis(TIPS-ethynyl)pentacene values corrected vs SCE.

(15) Balakrishnan, K.; Datar, A.; Oitker, R.; Chen, H.; Zuo, J. M.; Zang, L. *J. Am. Chem. Soc.* **2005**, *127*, 10496.

(16) Kang, S. J.; Bae, I.; Park, Y. J.; Park, T. H.; Sung, J.; Yoon, S. C.; Kim, K. H.; Choi, D. H.; Park, C. *Adv. Funct. Mater.* **2009**, *19*, 1609.

(17) Thin films of **4j** were inactive in OFETs, likely because of the morphology of the films and the dielectric interface.

(18) Chua, L. L.; Zaumseil, J.; Chang, J. F.; Ou, E. C. W.; Ho, P. K. H.; Sirringhaus, H.; Friend, R. H. *Nature* **2005**, *434*, 194.

(19) (a) Chen, Z. Y.; Lee, M. J.; Ashraf, R. S.; Gu, Y.; Albert-Seifried, S.; Nielsen, M. M.; Schroeder, B.; Anthopoulos, T. D.; Heeney, M.; McCulloch, I.; Sirringhaus, H. *Adv. Mater.* **2012**, *24*, 647. (b) Zaumseil, J.; Sirringhaus, H. *Chem. Rev.* **2007**, *107*, 1296.

(20) We tested only **4j** because it readily grew crystals, but the HOMO/LUMO levels of the other diaryl-IFs indicate that these too will be active in OFETs, research on which is ongoing.

(21) (a) de Boer, R. W. I.; Stassen, A. F.; Craciun, M. F.; Mulder, C. L.; Molinari, A.; Rogge, S.; Morpurgo, A. F. *Appl. Phys. Lett.* **2005**, *86*, No. 262109. (b) Takahashi, T.; Takenobu, T.; Takeya, J.; Iwasa, Y. *Appl. Phys. Lett.* **2006**, *88*, No. 033505.